

A Bound on Vorticity

Brett McInnes

National University of Singapore

email: matmcinn@nus.edu.sg

ABSTRACT

When nuclei collide peripherally at relativistic velocities, a Quark-Gluon Plasma may be formed with much larger values of vorticity than in any other known physical system: the STAR collaboration has reported observations of global polarization of Λ and $\bar{\Lambda}$ hyperons, generated in such collisions, corresponding to a value of the local angular velocity about $9 \pm 1 \times 10^{21} \cdot \text{s}^{-1}$ (averaged over impact energies). We show that, in a gauge-gravity model of QGP vorticity, one should nevertheless expect the vorticity to be bounded above in a collision with a given collision energy and centrality; furthermore, this bound is by a quantity which *decreases* with increasing impact energy. That is, the prediction is that QGP vorticity should be suppressed in collisions at high energy, and one should only expect to see evidence of it in the lower-energy collisions studied in the various Beam Energy Scans. *This apparently paradoxical prediction is in fact supported by observational data.* The bound is approximately attained in the cases where hyperon polarization is observable; if this is always the case in such experiments, then the model agrees with recent suggestions that these observations are related to a strong dependence of the plasma moment of inertia on impact energy.

1. How Vortical Can The QGP Be?

Very general considerations [1–9] indicate that sufficiently energetic peripheral heavy-ion collisions generate Quark-Gluon Plasmas (QGP) with substantial vorticities. This was predicted to be observable in the form of global polarization of Λ and $\bar{\Lambda}$ hyperons, and indeed the STAR collaboration [10] at the RHIC facility has announced [11] the first direct experimental data of this kind: for discussions see for example [12–19].

This major discovery has an unusual history. For these observations were not the first in which evidence of this effect were sought: in [20] the STAR collaboration itself reported such an attempt, involving collisions at energies considerably *higher* ($\sqrt{s_{\text{NN}}} = 62.4$, 200 GeV) than those employed in the more recent experiments. *No* statistically significant polarization effect was observed at that time. Similarly, such an effect has *not* been seen at the still higher collision energies studied in the ALICE experiment at the LHC [21]. In other words, it seems that the polarization is only observed at (relatively) *low* impact energies, typically around 39 GeV or below¹. This very remarkable observation means that vorticity could be a major topic of investigation for experiments involving relatively low impact energies, such as the NA61/SHINE experiment [23] and of course the *Beam Energy Scan* programmes [24, 25] being conducted at various facilities [26–28, 10], which will be reporting further data in the future.

The angular momentum imparted to the plasma in high impact energy collisions is undoubtedly much larger than in their low-energy counterparts². The apparently paradoxical observation that hyperon polarization is nevertheless only observable at low impact energies is currently a matter of intense theoretical interest: see for example [29, 30, 7, 12–14, 17, 31–35]. Several explanations have been proposed, including the “depolarizing” effects of higher temperatures in higher energy collisions [29], a possible strong effect of higher energies on fluid moments of inertia [30], longer lifetime of the fluid phase in the high energy case (leading to a dilution of vorticity), subtle effects of high energy on the rapidity distribution of the plasma’s angular momentum [14], asymmetries in the fireball which are concealed by the higher rate of its expansion in the high-energy case [13, 33, 34], and so on; and it may well be that several or all of these effects (or indeed some entirely new phenomenon) play a role to various degrees.

Here we wish to propose that the observations and their explanations can be organised according to the following simple scheme. It is intuitively clear that there must be some *upper bound* on the vorticity in a sample of any fluid, since its centrifugal effect will tend to disrupt the vortex itself. It is therefore natural to seek some understanding of our problem in terms of such a “*vorticity bound*” on the vortical QGP.

Some perspective on this situation is provided by the remark of Keane [27] that, in view of the extremely small size of these systems and the fact that they are produced in the aftermath of collisions at speeds extremely close to the speed of light, it is not surprising that angular velocities on the order of $10^{22} \cdot \text{s}^{-1}$ are produced. Elaborating on

¹A similar pattern has been predicted [22] for collisions of nuclei other than gold and lead, for example for copper-copper collisions.

²The angular momentum can be computed, using specific models of the nucleus, from the impact parameter of the collision; this in turn is deduced by means of the concept of *centrality*. “Centrality $p\%$ to $q\%$ ”, $p < q$, means that $p\%$ of collisions produce more tracks observed in the detector of a given experiment than the collisions under consideration, while $q\%$ produce fewer.

this, we note that, for a disc of radius (say) 1 femtometre, such an angular velocity (which is in any case an over-estimate for most collisions) corresponds to a maximal tangential velocity less than one-tenth of the speed of light. Even allowing for the effects of viscosity, which in any case is generally described as “small” (see [36] for an attempt to be precise about this), from this point of view one could argue that the observed vorticity is actually rather *small* for a system of this size.

In summary, it appears not only that QGP vorticity is unobservable in very high energy collisions, but that it is not particularly large even in relatively low-energy collisions. This is consistent with the fact that it has been so hard to detect; equally, it is consistent with the idea that there is some kind of restrictive upper bound on this vorticity.

2. A Vorticity Bound From Holography

The experimental evidence for QGP vorticity was discovered at the RHIC facility by lowering the impact energies in convenient steps (to be described). As with the other Beam Energy Scan experiments mentioned earlier, this takes us into the realm of very strongly coupled plasmas. It also takes us into an unfamiliar region of the quark matter phase diagram, a region of large baryonic chemical potentials, and also of extremely intense magnetic fields [37–43] induced in the plasma by the spectator nucleons (this could be relevant here because of possible non-trivial interactions between magnetic fields and vorticity: see for example [44, 45]). To analyse the behaviour of the vortical QGP, we therefore need technical tools capable of handling strong coupling, large baryonic chemical potentials and magnetic fields, and so on.

In this domain, the techniques of *gauge-gravity duality* [46–48] (“holography”) are suitable, and they have played the useful role of directing attention to features of the QGP that might otherwise have escaped attention. The method is particularly valuable in suggesting the existence of certain *bounds* on important quantities: most famously, it imposes, under well-understood circumstances, a (lower) bound on the plasma’s dynamic viscosity, a bound which depends on its entropy density but also on other physical parameters [49–52]. Other examples involve parameter-dependent bounds on cosmic magnetic fields [53] and on the QGP Reynolds number [36].

The simplest holographic models of the QGP involve thermal black holes in an asymptotically AdS spacetime: the physics at infinity should correspond, at least qualitatively and perhaps to some extent quantitatively, to the physics of the QGP. In the case where the system at infinity has a large angular momentum, holographic duality requires that the bulk black hole should itself have a non-zero angular momentum: it must be a (magnetically and electrically) charged version of the AdS-Kerr-Newman metric (first used in this general context in [54].) The angular momentum and angular velocity of the black hole represent (in a highly non-trivial way) the corresponding quantities for matter on the boundary, which models the QGP vortices we wish to study.

There are two questions to be considered here. First, can a holographic model be consistent, even at a qualitative level, with the suppression of hyperon polarization in the QGP at high impact energies and angular momenta? It seems hard to imagine that this is possible: yet, if the method were inconsistent with the observations of this (possibly fundamental) property of the QGP, it would call into question the entire programme of

applying gauge-gravity duality to these systems. Secondly, if the gauge-gravity approach somehow passes this test, can it provide a precise mathematical formulation of the “vorticity bound” we suggested earlier as a way of understanding this strange phenomenon?

Even in the simplest models (which are nevertheless fully adequate for analysing present data, as in [11]), the polarization percentage is proportional not only to the vorticity, but also, inversely, to the temperature: see equation (26), below. This does not, however, solve the problem: as impact energies increase, so do temperatures, but only very slowly — far too slowly to account for the effect we are discussing here. In these models, then, one has to look for an explanation in terms of the behaviour of the QGP vorticity itself: it must (*in effect*) vary in some unusual (non-linear) way as the impact energy — and, with it, the angular momentum imparted to the plasma — increase. (A non-linear relation between angular momentum and angular velocity is possible, but only if the moment of inertia of the plasma sample is affected by the impact energy, as suggested in general terms in [30]; related ideas have been put forward in [13, 33, 34].)

The crucial point here is that, in the physics of rotating black holes, *there is in fact a highly unusual relationship between the angular momentum and the angular velocity of particles moving around the black hole*, connected with the well-known phenomenon of frame dragging. This relation is certainly non-linear (zero angular momentum does not entail zero angular velocity, for example). Thus we can hope that the gauge-gravity duality might supply the relation we need here.

We stress that we are not suggesting that QGP vortex angular velocities are in fact related to their angular momenta in precisely the way we deduce below, just as, when using holography generally, one does not claim that a conformal field theory is a fully realistic representation of QCD. The suggestion is that it could be useful to have an *explicit*, mathematically derived formula of this kind, representing the physical effects actually responsible for the observed decrease of polarization with increasing impact energy (as discussed in the references listed above). Such a formula might be interesting if it points to some previously unknown aspect of QGP physics; in particular, it will be useful if it leads us to a concrete mathematical formulation of the vorticity bound we seek.

We will show that the simple holographic model based on the geometry of an AdS-Kerr-Newman black hole spacetime actually realises this programme. It leads directly to an explicit formally non-linear relation between vorticity and angular momentum, which does in fact impose an *upper bound* on the possible vorticity in a boundary theory that represents the QGP produced by a heavy-ion collision with a given impact energy and centrality. The bound takes the explicit and simple form

$$\omega \leq \varkappa \frac{\varepsilon}{\alpha} \approx 0.3487 \frac{\varepsilon}{\alpha}, \quad (1)$$

where ω is the vorticity (equal to the local angular velocity in the convention, used here, in which vorticity is half the curl of the velocity field³), ε is the energy density of the plasma, α is its angular momentum density, and \varkappa is a certain dimensionless constant with the indicated approximate value⁴. The two densities can be computed from the impact energy

³Note that many references define it as the curl itself, but here we follow [8] and [11].

⁴The exact value is $\varkappa = \varsigma^{-1} \sqrt{\frac{\varsigma^2 - 1}{\varsigma^4 + \varsigma^2 - 1}}$, where $\varsigma = \sqrt{\frac{1}{3} \left(1 + \Re \left([-10 + 6\sqrt{111}i]^{1/3} \right) \right)}$, where \Re denotes the real part and the cube root is taken to lie in the first quadrant.

and the centrality of the collision, as explained earlier, and so one can think of the bound as being fixed by those data⁵.

This upper bound is remarkable in three ways. First, it depends only on two readily computed quantities, ε and α , and only on their *ratio*: each of these quantities, as a density, varies strongly as the fireball explodes, but their ratio is much less affected.

Secondly, as we will see, the derivation follows in a quite elementary way from the structure of the geometry imposed on conformal infinity by the bulk black hole geometry, without any further assumptions: it does not, for example, depend on subtle stability analyses like those employed to derive the bounds in [53] and [36]. Its status as a prediction of the gauge-gravity duality is correspondingly robust.

Finally, and most importantly: if we fix the centrality but increase the impact energy, both ε and α increase; *but α increases far more rapidly than ε* , so, since the right side of (1) depends on α inversely, the bound becomes ever more stringent as the impact energy increases. In particular, as we will show, the bound reduces the vorticity below any observable level for high-energy collisions (say, 62.4 GeV and higher). On the other hand, the bound is much less stringent at lower impact energies, and (allowing for the large theoretical and observational uncertainties) permits observable hyperon polarization at impact energies around 39 GeV or lower. This is, of course, precisely the kind of behaviour that is observed and that the gauge-gravity duality must (roughly) reproduce.

We find, comparing with the data reported in [11], that our bound is satisfied, in fact approximately *attained*, in all cases except one, where the impact energy is so low that it is questionable whether a plasma is in fact actually produced. We will show that, if we assume that the bound is attained, then the model gives an explicit account of the *changes in the plasma moment of inertia* that explain how the angular velocity can be small at high impact energies.

A useful way of thinking about the vorticity bound is that it tells us precisely what it means, for collisions at a given impact energy and centrality, to say that the resulting vorticity is “large”: it means that the vorticity is of the order of the value on the right side of the inequality (1). We will show that the vorticities reported in [11] are certainly large in this sense. Since these vortices are sustained by the strong(est) interaction, it may be that these reported values are the largest possible (in this sense) for vortices in *any* substance.

We begin by setting up the holographic model. (Note that this was done in much more detail, though to a different purpose, in [55].)

⁵We shall use, throughout, natural units; however, since most of the parameters have interpretations in terms of lengths and volumes, it is convenient to take as our base unit the femtometre or fm (1 fm⁻¹ \approx 197.327 MeV). Then ω has units of fm⁻¹, ε has units of fm⁻⁴, and α has units of fm⁻³. More familiar units for ω can be restored by multiplying by $c = 3 \times 10^{23}$ fm·s⁻¹.

3. The Holographic Model

The bulk metric here [56] is that of an asymptotically AdS rotating black hole with a topologically spherical event horizon (the “dyonic” AdS-Kerr-Newman metric):

$$g(\text{AdSdyKN}) = -\frac{\Delta_r}{\rho^2} \left[dt - \frac{a}{\Xi} \sin^2 \theta d\phi \right]^2 + \frac{\rho^2}{\Delta_r} dr^2 + \frac{\rho^2}{\Delta_\theta} d\theta^2 \quad (2)$$

$$+ \frac{\sin^2 \theta \Delta_\theta}{\rho^2} \left[a dt - \frac{r^2 + a^2}{\Xi} d\phi \right]^2,$$

where

$$\begin{aligned} \rho^2 &= r^2 + a^2 \cos^2 \theta, \\ \Delta_r &= (r^2 + a^2) \left(1 + \frac{r^2}{L^2} \right) - 2Mr + \frac{Q^2 + P^2}{4\pi}, \\ \Delta_\theta &= 1 - \frac{a^2}{L^2} \cos^2 \theta, \\ \Xi &= 1 - \frac{a^2}{L^2}. \end{aligned} \quad (3)$$

Here the coordinates are generalized Boyer-Lindquist coordinates (with θ and ϕ having the usual angular ranges), $-1/L^2$ is the asymptotic sectional curvature⁶, and a is the angular momentum per unit physical mass (always taken to be non-negative); M , Q , and P are parameters which describe the black hole geometry and which are related to the physical mass, electric charge, and magnetic charge of the hole by [57]

$$m = M/(\ell_{\mathcal{B}}^2 \Xi^2), \quad q = Q/(\ell_{\mathcal{B}} \Xi), \quad p = P/(\ell_{\mathcal{B}} \Xi), \quad (4)$$

where $\ell_{\mathcal{B}}$ is the gravitational length scale in the bulk. Notice that we must have

$$a/L < 1, \quad (5)$$

since otherwise the signature will fail to be Lorentzian near to the poles.

The physics of this black hole determines, according to the gauge-gravity duality, that of a field theory on the boundary ($r \rightarrow \infty$); the latter corresponds, to some extent, to the QGP. Thus, the Hawking temperature T of the black hole corresponds to the temperature of the plasma, the electromagnetic field surrounding the black hole determines the magnetic field B experienced by the plasma and also its baryonic chemical potential μ_B ; the ratio of the black hole’s entropy to its (physical) mass is equal to the ratio of the plasma entropy density s to its energy density ε , and similarly the black hole parameter a is interpreted as the ratio of the QGP angular momentum density to its energy density.

Conversely, given these quantities, *together with the bulk curvature parameter L* , one can reconstruct the black hole geometry (that is, the four parameters $M, Q, P, \ell_{\mathcal{B}}$) by

⁶In order to ensure that this parameter will not be confused with the angular momentum, we refer to the latter, under all circumstances, only through the parameter a .

solving the following four⁷ equations (see [55] for the derivations):

$$T = \frac{r_h \left(1 + a^2/L^2 + 3r_h^2/L^2 - \frac{a^2 + \{Q^2 + P^2\}/4\pi}{r_h^2} \right)}{4\pi(a^2 + r_h^2)}, \quad (6)$$

$$\frac{s}{\varepsilon} = \frac{\pi \Xi (r_h^2 + a^2)}{M}, \quad (7)$$

$$B = \frac{\Xi P}{\ell_B L^2}, \quad (8)$$

$$\mu_B = \frac{3(Qr_h + aP)}{4\pi\ell_B(r_h^2 + a^2)}, \quad (9)$$

where r_h is the value of the radial coordinate at the outer horizon; it is determined by the black hole parameters (provided, again, one knows L) in the usual way, by setting $\Delta_r(r_h) = 0$.

We record these equations here in order to stress two points. First, we see that the formalism is quite capable of handling the novel physical conditions that will be encountered in the future Beam Energy Scans. These conditions may however lead to unfamiliar behaviour. For example, if a is very large, then (because of the presence of the Ξ factor in equation (8)) P could be unexpectedly large even if B is rather small; we then see from equation (9), where the term aP occurs in the numerator, that even a relatively small magnetic field can strongly influence the computation of the baryonic chemical potential if the angular momentum is large. That is, magnetic fields and angular momentum can interact non-trivially in this context, and this may prove to be important in experiments in which μ_B can be very large.

Secondly, these formulae allow us to see explicitly that the “holographic dictionary” depends on having a physical basis for choosing the parameter L . This quantity is of fundamental geometric importance in the bulk: it determines what the bulk curvature would be in the absence of the black hole⁸. Its precise physical meaning, however, is less clear. There is an extensive literature (for example, see [59–61]) on the interpretation of the AdS cosmological constant $-3/L^2$ as defining a pressure $3/(8\pi\ell_B^2 L^2)$, with a consequent (very subtle) interpretation in terms of the pressure of the matter in the boundary theory. While it would certainly be of interest to pursue this as a way of determining L given physical data, here we will proceed in a more direct way, by showing that L mediates the relationship between the angular momentum of the boundary theory and the corresponding angular velocity.

⁷This is correct in principle; but, in practice, the situation is far more complicated, because on physical grounds one expects the entropy density to be strongly affected by vorticity, since the latter can be expected to restrict the phase space in a similar manner to the magnetic field [58]. Thus we do not really “know” s here even if we do know it in the non-rotating case. See [55] for a discussion as to how to deal with this.

⁸Note that there is no scaling symmetry here, as there is for asymptotically AdS black holes with (topologically) planar event horizons.

4. Vorticity and Angular Momentum in the Holographic Model

As with the asymptotically flat Kerr-Newman geometry, the bulk geometry here is characterized by the remarkable phenomenon of *frame dragging*. There is a fundamental difference between the two, however, and this proves to be crucial for our purposes; so let us briefly review how frame dragging works in our case.

Consider a free particle (always with non-zero rest mass, henceforth) in the AdS-Kerr-Newman spacetime. Because this spacetime, unlike the Schwarzschild spacetime, does not have a symmetry in the θ direction, even free particles can have complicated orbits; so we will (throughout) focus on particles on or near the equator. This allows us to set θ equal to a fixed constant, $\pi/2$. We can then focus on angular momentum associated with the ϕ direction, which is all we need to set up a model of vorticity in the QGP.

Recall now that, in a spacetime like this one which is not flat, angular momentum is not defined by the familiar formula which makes it proportional to the angular velocity; for that quantity would not, in general, be conserved for a free particle even in the presence of a rotational symmetry.

Instead one proceeds by noting that an angular Killing vector field — in this case the one associated with the ϕ direction, normalised so that ϕ has period 2π — allows us to define, along the geodesics corresponding to free particles, a conserved quantity. This is the angular momentum per unit mass: the inner product of this normalised Killing field with the unit tangent to the particle worldline, $i\partial_t + \dot{\phi}\partial_\phi$ (where dots denote differentiation with respect to the proper time of the particle).

Thus, for a massive particle on the equator, outside the event horizon, with *zero* angular momentum, we have (from equation (2))

$$\frac{a}{\rho^2\Xi} (\Delta_r - [r^2 + a^2]) \dot{t} + \frac{1}{\rho^2\Xi^2} \left(-a^2\Delta_r + [r^2 + a^2]^2 \right) \dot{\phi} = 0, \quad (10)$$

and so the angular velocity of such a particle relative to this system, Ω_0 (the subscript referring to the angular momentum per unit mass), takes the value

$$\Omega_0 = \frac{d\phi}{dt} = \left(\frac{1 - \frac{r^2+a^2}{\Delta_r}}{a^2 - \frac{[r^2+a^2]^2}{\Delta_r}} \right) a\Xi. \quad (11)$$

This is non-zero in general, and so we have the phenomenon of frame dragging: *even a particle with zero angular momentum has a non-zero angular velocity* in general.

The great difference between the asymptotically flat and asymptotically AdS cases, however, is that frame dragging in the latter case is omnipresent: even at arbitrarily large distances from the black hole, one still has a residual angular velocity (denoted by ω_0), obtained by letting $r \rightarrow \infty$ in (11) (note that Δ_r is asymptotic to r^4/L^2):

$$\omega_0 = \frac{-a}{L^2}. \quad (12)$$

This does not happen in the asymptotically flat case, and it represents an important departure. For it means that the rotation of the black hole leaves, in the AdS case, a

direct physical imprint on the region “near infinity”. When we construct the conformal boundary, as we need to do to use holography⁹, we must take this into account.

The geometry of this boundary is fixed by means of a conformal re-scaling of the metric $g(\text{AdSdyKN})$ as the limit is taken to infinity. Mathematically we are entitled to use any conformal factor with the appropriate asymptotic behaviour, and clearly there is a wide choice of representatives of the conformal structure at infinity so defined; in fact, in this case the conformal boundary is conformally flat, since its Cotton tensor vanishes. From a physical point of view, however, it makes sense to choose a representative which reflects the persistence of frame dragging to points in the spacetime arbitrarily distant from the black hole.

With this in mind, we take the boundary metric to be

$$g(\text{AdSdyKN})_\infty = -dt^2 - \frac{2a \sin^2\theta dt d\phi}{\Xi} + \frac{L^2 d\theta^2}{1 - (a/L)^2 \cos^2\theta} + \frac{L^2 \sin^2\theta d\phi^2}{\Xi}, \quad (13)$$

obtained from $g(\text{AdSdyKN})$ by extracting a conformal factor r^2/L^2 , taking the limit $r \rightarrow \infty$, and then doing some algebraic simplifications.

Notice that, with this metric, the time coordinate t represents proper time for a stationary observer at infinity located at one of the poles ($\theta = 0$); we can take this observer to be an outside observer, fixed in the laboratory; so, in each case we consider below (particles with zero, respectively non-zero angular momentum), $d\phi/dt$ represents an angular velocity as measured by this observer. Notice too that a massive particle on the equator moving with angular velocity ω_0 has, as the notation suggests, zero angular momentum: from equation (13), the angular momentum per unit mass is

$$\frac{\dot{t}a}{\Xi} + \frac{\dot{\phi}L^2}{\Xi} = \frac{\dot{t}}{\Xi} (a + \omega_0 L^2) = 0, \quad (14)$$

so, with this choice of metric, the angular velocity at infinity matches the residual frame dragging angular velocity in the bulk. One might say that “the space at infinity is rotating” at a constant angular velocity, but this is slightly misleading: we should bear in mind that it means no more than that ω_0 is the angular velocity of massive particles having angular momentum per unit mass equal to *zero* (and *not* to a).

We propose to use the spacetime with metric $g(\text{AdSdyKN})_\infty$ to connect the rotation of the bulk black hole with the angular momentum of the plasma in a QGP with non-zero vorticity. As usual in collision physics, the matter produced by the collision is described by focusing on a two-dimensional *reaction plane* or “ $x-z$ plane” containing the axis of the collision (conventionally denoted z), a perpendicular axis measuring distance away from the axis (conventionally denoted by x) and a y axis pointing in the approximate direction of the angular momentum vector. We regard the QGP vortices as inhabiting the reaction plane, so we focus exclusively on that plane. In effect the spacetime is, including a time coordinate, three-dimensional. Thus the use of a three-dimensional spacetime in the holographic model is appropriate.

Before we can use our boundary space, however, we need to deal with the fact that this spacetime is not flat. We already understand the non-diagonal term in the metric: it arises simply because the angular momentum of the black hole leaves a direct imprint

⁹For the AdS/CFT duality in this situation see [62].

on infinity, in the form of frame dragging. By definition, frame dragging involves a highly unusual relation between angular momentum and angular velocity, and this is precisely what we are seeking, as explained in Section 2 above.

Less welcome is the fact that the spatial sections at infinity are not flat: they have the topology of a two-sphere, endowed with a specific non-flat geometry (which is not that of a round sphere of radius L , unless of course $a = 0$). We are particularly interested in the region near to the equator, where we propose to locate the matter that will model the plasma; we need to convince ourselves that this region is not strongly affected by the curvature of the space there.

The Gaussian curvature of the spatial sections is given by

$$K(\theta) = \frac{1}{L^2} \left(1 - 2 \frac{a^2}{L^2} \cos^2 \theta \right). \quad (15)$$

We see immediately that, near the equator¹⁰, the curvature remains near to its value in the non-rotating case, $+1/L^2$.

In practice, the quantity a , identified holographically as the ratio of the boundary matter’s angular momentum density to its energy density, is usually quite large relative to the length scales of this system: for example, for collisions of gold ions at 200 GeV and 20% centrality (see below), the value for the resulting plasma is about 82.5 fm. The inequality (5) means that L is at least as large (so one cannot think of it as defining the length scale of a fluid vortex, which is much smaller); so $K(\pi/2) = 1/L^2$ is always very small relative to the relevant length scales. We will confirm this, in detail, below. In short, the curvature of the spatial sections is too small to affect our modelling¹¹.

To resume: we have seen that, due to the frame dragging effect inherited at infinity from the bulk black hole, a particle with zero angular momentum there rotates relative to the coordinate system we used above. Here, however, we are not concerned with matter having *zero* angular momentum: by hypothesis, the angular momentum of the vortical QGP is some *non-zero*, in fact large, value. The obvious way to represent this in our model is to consider particles on the equator not with zero angular momentum, but rather with an angular momentum to mass ratio given precisely by a , the ratio of the QGP angular momentum density to its energy density. These will of course rotate not at ω_0 but at a different angular velocity, ω_a , relative to this coordinate system.

The physical angular velocity ω is computed as the difference between the angular velocity of particles with non-zero angular momentum and that of the space itself (visualised in terms of fictitious particles with zero angular momentum), $\omega = \omega_a - \omega_0$. This

¹⁰Near to the poles, by contrast, the curvature of the “sphere” will actually be *negative* provided that $a/L > 1/\sqrt{2}$, a condition that is easily satisfied in this context, as we will see later. (We are particularly interested in the case of $a/L = 1/\zeta$ (see equation (23) below); we have $1/\zeta \approx 0.83 > 1/\sqrt{2} \approx 0.71$.)

¹¹As a matter of fact, QGP vortices, as systems rotating at relativistic velocities, are akin to a system well known to historians of physics: the *relativistic rotating disc* (the subject of the “Ehrenfest paradox”). Such a disc *does* in fact have non-zero (actually, negative) Gaussian curvature (as seen by observers fixed in position on the disc). See [63], page 90, for a clear modern treatment. The curvature of the relativistic rotating disc (if it is “Born rigid”, which may not in fact be the case here) is negligible in the case of QGP vortices, since one expects it to be of the order of the square of the angular velocity (which, as we will see, is very small in units of (inverse) femtometres, which correspond to the physical length scale of this system). In this sense, the assumption that the space inhabited by a QGP vortex is flat may itself be an approximation (though a good one); so our procedure here is not as peculiar as it may appear.

will correspond to the vorticity of the plasma observed in the laboratory. (ω_0 and ω_a , by contrast, do not correspond to anything observable and should be regarded as mere formal constructs.)

We now proceed precisely as in the computation of frame dragging. Again we evaluate the conserved quantity, the inner product of the unit tangent with the normalised Killing vector field, but now we have

$$\frac{\dot{t}a}{\Xi} + \frac{\dot{\phi}L^2}{\Xi} = a. \quad (16)$$

The situation now is a little more complicated than before, since this equation cannot be solved for $\omega_a = d\phi/dt$ directly; we need also to use the fact that $\dot{t}\partial_t + \dot{\phi}\partial_\phi$ is indeed a unit vector, that is,

$$-\dot{t}^2 + \frac{2\dot{t}\dot{\phi}a}{\Xi} + \frac{\dot{\phi}^2L^2}{\Xi} = -1. \quad (17)$$

Using this equation, we can eliminate \dot{t} , so obtaining a quadratic equation for ω_a :

$$L^2\omega_a^2 + 2a\omega_a + \frac{a^2}{L^2} \left(1 - \frac{\Xi}{1 + \frac{a^2}{L^2}\Xi} \right) = 0. \quad (18)$$

Solving this and subtracting ω_0 , we obtain two equal and oppositely signed values for ω , corresponding of course to the two possible directions of rotation; taking the positive value we have finally, recalling the definition of Ξ ,

$$\omega = \frac{a}{L^2} \sqrt{\frac{1 - \frac{a^2}{L^2}}{1 + \frac{a^2}{L^2} \left(1 - \frac{a^2}{L^2} \right)}}. \quad (19)$$

We see that the relation between angular velocity and angular momentum (per unit mass) is not simple in this model; the two are *not* proportional unless a/L is known to be very small and L is fixed. In fact we see that ω is *small* when a is large (approaching L)¹². In short, equation (19) supplies the promised formal non-linear relation which we hope to use to codify the peculiar fact that, observationally, large angular momenta do not seem to lead to large hyperon polarizations.

The specific form of the right side of equation (19) can be understood by computing the linear velocity of points on the equator. From equation (13) we see that the circumference is $2\pi L/\sqrt{\Xi}$ (which is very large, much larger than $2\pi L$, when a is close to L). For an angular velocity ω , the linear velocity is therefore

$$v_{\text{eq}} = \frac{\omega L}{\sqrt{1 - \frac{a^2}{L^2}}}, \quad (20)$$

and this will exceed unity as a approaches L *unless* ω tends to zero sufficiently rapidly in the same limit. In short, the angular velocity must decrease towards zero as the angular momentum increases in order to avoid violating causality. In fact, substituting equation (19) into (20) we find

$$v_{\text{eq}} = \frac{a}{L} \frac{1}{\sqrt{1 + \frac{a^2}{L^2} \left(1 - \frac{a^2}{L^2} \right)}}, \quad (21)$$

¹²One should take care not to think of L as a ‘‘constant’’ under all circumstances: in our later work, it depends on the impact energy, for example, and so is not independent of a .

and (in view of inequality (5)) this does always satisfy causality, because the factor of $\sqrt{\Xi}$ has been cancelled.

Let us consider the origin of the crucial quantity Ξ . It appears in the final term in equation (13) simply because it is inherited from the black hole metric in equation (2). In both cases it is necessarily present in order to ensure that the geometry should be regular: without it, there would be conical singularities at the poles (that is, the ratio of the circumference of a circle centred on a pole to its radius would not tend to 2π as the radius tends to zero¹³).

To summarize, then: due to the (geometrically necessary) presence of the Ξ factor, the length of the equator in this geometry depends on the angular momentum, and this, via the requirement of causality, enforces a non-linear relation between angular velocity and angular momentum. This in turn allows ω to approach zero as a becomes large relative to L . This seems odd on one side of the holographic duality, but by no means on the other; for it is obvious that the Kerr-like bulk geometry does change in response to changes in the angular momentum of the black hole. Equally, the holographic duality reconciles us to the possibility that angular momentum need not be linearly related to angular velocity, for, around a black hole, this is precisely the normal situation.

Equation (19) has several important consequences. First, it allows us to compute or estimate the elusive parameter L : for example, if one has observational data on the vorticity produced in the plasma by collisions at given impact energy and centrality (so that the angular momentum can be computed), then (19) allows the value of L to be deduced under those conditions. A similar calculation can be done if one has theoretical estimates for ω (see for example [30]). Alternatively one might try a more phenomenological approach, by postulating some simple relation between L and a directly, guided by the need to ensure that the inequality (5) is always satisfied. In any case, as we saw in the preceding Section, once L is fixed, the full holographic dictionary can be used.

Secondly, equation (19) gives us some insight as to the physical meaning of L , in this particular application, in terms of the boundary physics (without relying on its meaning in the bulk). One can think of the right side of (19) as a product of a/L^2 with the “holographic correction” involving a^2/L^2 . If we leave aside this correction, then this would identify L^2 as the moment of inertia of the system per unit mass. That is, L itself would correspond to the classical *radius of gyration*, the quantity that describes the distribution of the rotating matter relative to the axis of rotation (which may vary with time or, as we will see, with the impact energy); so, with the correction included, one might think of L as a “generalized radius of gyration”. We can therefore think of changes in L as having a physical meaning in terms of changes in the distribution of the plasma around the axis of a vortex. We will return to this later.

All this has the unfortunate consequence, however, that it seems that we cannot apply the holographic formula (19) to understand the STAR collaboration data, since we need to use those data to determine L . Fortunately, there is a simple way to circumvent this problem.

¹³This is particularly clear in the boundary geometry: there, the circumference of a circle of the form $\theta = \theta_0 = \text{constant}$ is $2\pi L \sin \theta_0 / \sqrt{\Xi}$, while its radius is $L \int_0^{\theta_0} d\theta / \sqrt{1 - (a^2/L^2) \cos^2 \theta}$, and the ratio only tends to 2π as $\theta_0 \rightarrow 0$ because the $\sqrt{\Xi}$ factor is present.

5. The Bound

As we know, the black hole parameter a has a holographic interpretation as the ratio of the plasma angular momentum density to its energy density; it can therefore be computed explicitly from physical data, and we will explain how to do this shortly. Knowing a , we may use equation (19) to regard ω as a function of L . We know (from the inequality (5)) the domain on which L can vary: it is the open interval (a, ∞) . We now ask more specifically: for a given value of a , how does ω behave, as a function of L , on this domain?

Equation (19) answers this question. Clearly ω vanishes as $L \rightarrow \infty$, as expected, since this is the regime of small angular momentum per unit mass (or of large radius of gyration, as above). More surprisingly, we have seen that it *also* vanishes as L tends to a . Now since ω is continuous and positive as a function of L , *it follows that ω is bounded above.*

In fact, $\omega(L)$ can be completely described analytically; the analysis is rather intricate but of course essentially elementary¹⁴. One finds that this function has a unique maximum, ω_{\max} , at $L = L_{\omega_{\max}}$, given by

$$L_{\omega_{\max}} = \varsigma a, \quad (22)$$

where ς is a pure number given by

$$\varsigma = \sqrt{\frac{1}{3} \left(1 + \Re \left(\left[-10 + 6 \sqrt{111} i \right]^{1/3} \right) \right)} \approx 1.2048, \quad (23)$$

\Re denoting the real part and the cube root being the one such that its real and imaginary parts are both positive.

We can now compute ω_{\max} as

$$\omega_{\max} = \frac{1}{\varsigma a} \sqrt{\frac{\varsigma^2 - 1}{\varsigma^4 + \varsigma^2 - 1}} \equiv \frac{\varkappa}{a} \approx \frac{0.3487}{a}, \quad (24)$$

where \varkappa is defined in terms of ς in the manner shown. That is, *no matter how* L is determined by the underlying physical effects, ω can never exceed this value, once a has been fixed. With the holographic interpretation of a as α/ε , this is the bound given in Section 2 above.

An example is shown in Figure 1: this shows $\omega(L)$ in the case of collisions at 27 GeV per pair, with 20% centrality (see below for the details). Here $\alpha/\varepsilon \approx 19.94$ fm; there is a clear maximum at $L \approx 24.02$ fm; and the value of ω at that maximum is ≈ 0.0175 fm⁻¹, in agreement with (22) and (24).

To summarize: we have proposed that the observed data can be described formally by a non-linear relation between vorticity and angular momentum. The gauge-gravity duality provides an *explicit* relation of this kind: equation (19). If this equation does describe the situation more or less accurately, then it follows that QGP vorticities are bounded above, as in equation (24).

¹⁴One computes the derivative and sets it equal to zero; a somewhat elaborate algebraic manipulation reduces this condition to $L^6 - a^2 L^4 - a^4 L^2 + (a^6/2) = 0$, which is a cubic in L^2 and can consequently be solved explicitly (leading to the odd-looking solution involving the number 111). The sextic in L has two complex solutions, two negative real solutions, one real positive solution which however violates (5), and one physically acceptable solution.

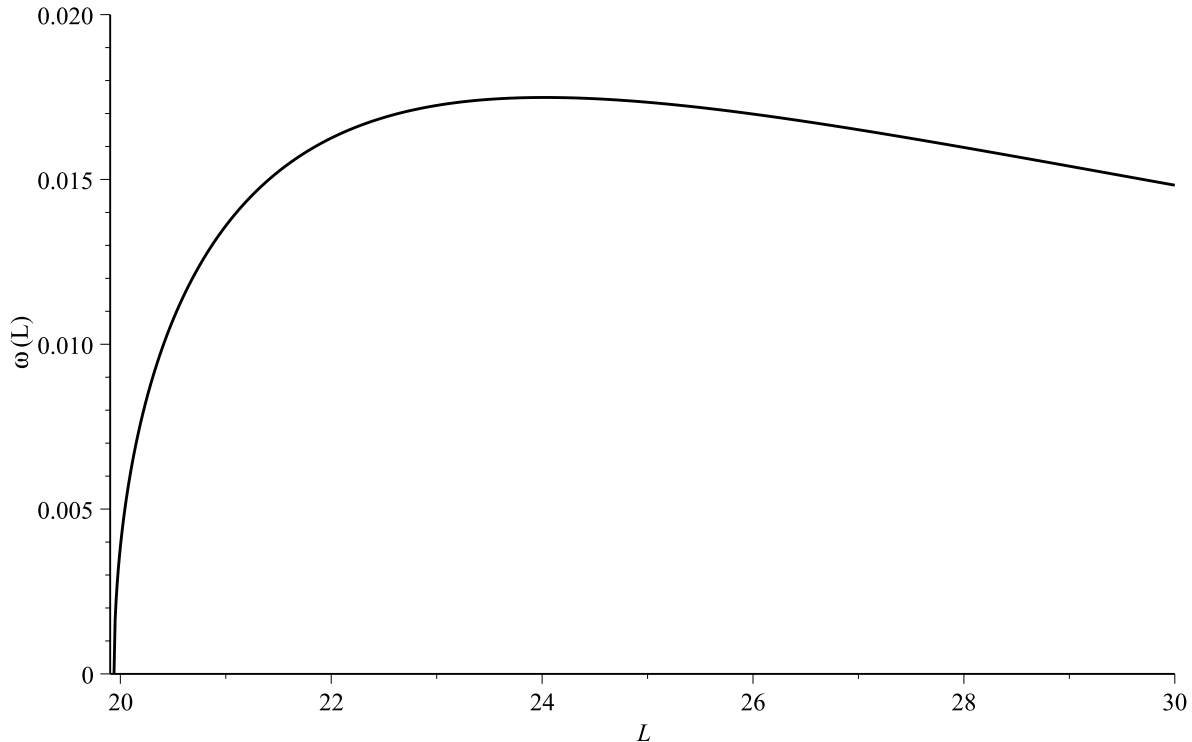


Figure 1: Angular velocity as a function of L , impact energy 27 GeV, centrality 20%.

Notice that, even when the equator is rotating at the maximal possible angular velocity for a given value of a , points on it move at a velocity $v_{\text{eq}}(\omega_{\text{max}})$, given (from equation (21)) by

$$v_{\text{eq}}(\omega_{\text{max}}) = \frac{1}{\sqrt{1 + \zeta^2 - \zeta^{-2}}} \approx 0.753, \quad (25)$$

that is, well below light speed. Thus causality does *not* explain the existence of the upper bound — an important point¹⁵.

Instead, the existence of the vorticity bound is ultimately due to the specific form taken by the black hole metric in the bulk, which involves factors of Δ_θ and Ξ (*not* occurring in the more familiar asymptotically flat Kerr-Newman metric) which must be present if the Einstein equation (with a non-zero cosmological constant) is to be satisfied and (as we saw earlier) conical singularities are to be avoided. The bound is in this sense truly a *holographic* bound.

We now turn to the problem of comparing this bound with the actual data (from [11]).

6. The Data

Before we begin, we should be open regarding the fact that precision is not to be looked for in these computations. As is well known, the field theories considered in the gauge-gravity duality are not (in all regimes) closely similar to QCD: there are important analogies

¹⁵Of course, in general, the question of causality can indeed be crucial in discussions of (sufficiently large) rapidly rotating systems: see for example [64] and references therein. The point is that this is not the case here.

(discussed very clearly in [46]) but there are basic differences. The observational data, too, suffer from large uncertainties: [11] reports a large systematic uncertainty in the given values of the polarization percentages. (The principal difficulty here is that, to relate vorticities, which are not directly observable, to polarizations, one needs to know the precise temperature corresponding to a given energy density; and this is a notoriously difficult problem [65].)

We will nevertheless see that there is much to be learned here; our main priority at this point, however, is to assure ourselves that the vorticity bound predicts values that are at least of a reasonable order of magnitude. Our secondary objective is to explain clearly how the relevant calculations can be done when more precise data become available in future.

We need estimates for the angular momentum of the QGP in peripheral collisions, and also for the energy density, for various impact energies and centralities. For the former, we rely on [30], where estimates¹⁶ using the AMPT (“A Multi-Phase Transport”) model are given; for the latter we use [66], where very detailed computations of many relevant parameters (using a colour string percolation model) are given. In both cases, the values given seem reasonable. Other models might be chosen, but the differences are unlikely to be sufficiently large as to modify our general conclusions.

Proceeding in this way, we can (with simple additional assumptions regarding the geometry of the overlapping nuclei) compute the right side of the inequality (1), and thus place an explicit bound on the vorticity in each case. We can relate this to the average polarizations of primary Λ and $\bar{\Lambda}$ hyperons by means of the equation¹⁷ (see [8] and [11])

$$\overline{\mathcal{P}}_{\Lambda'} + \overline{\mathcal{P}}_{\bar{\Lambda}'} = \frac{\omega}{T}, \quad (26)$$

where natural units are used and T is the temperature as usual. This equation allows us to express the vorticity bound as a bound on the total polarization, obtaining inequalities of the form

$$[\overline{\mathcal{P}}_{\Lambda'} + \overline{\mathcal{P}}_{\bar{\Lambda}'}] (\sqrt{s_{\text{NN}}}, C) \leq \Phi(\sqrt{s_{\text{NN}}}, C), \quad (27)$$

where C denotes centrality and where we now know how to compute $\Phi(\sqrt{s_{\text{NN}}}, C)$ from ω_{max} in each instance; it is expressed as a percentage.

We consider three different impact energy regimes.

6.1 Collisions at 62.4 GeV and Higher

Let us begin by considering the highest-energy collisions studied by the STAR collaboration and reported in [20], at 200 GeV per pair; that work also reports results on collisions at 62.4 GeV, to which we return below; we will also discuss the analogous LHC studies at that point.

In [11], the focus is on collisions with 20% to 50% centrality. This means [67, 68] that the impact parameters vary from around 6.75 femtometres (fm) up to around 10.5 fm. On this domain, one finds [30] that the angular momentum imparted to the plasma in 200

¹⁶Note that, in [30], the convention is used in which ω is twice as large as in [11] and here.

¹⁷The primes indicate that these are the polarizations for “primary” hyperons, which means that we are neglecting the “feed-down” effect; see [8] for the theory of this, and [11] for a discussion of its effect on the STAR observations.

GeV collisions steadily decreases, from about 110000 (in natural units; in conventional units, $110000 \cdot \hbar$) at $b = 6.75$ fm to around 40000 at $b = 10.5$ fm. However, the volume of the overlap region *also* decreases as the impact parameter increases, and we find that, to a good approximation, the two effects cancel for collisions with 20% to 50% centrality: that is, the angular momentum density α is roughly independent of b in this range of b values. We therefore focus on collisions at 20% centrality, since, in this range, these collisions are the least affected by the variations of the nuclear density near the boundary of the nucleus, and other effects associated with the very small volumes of the plasma produced by high-centrality collisions.

We follow [69] in taking the shape of the nucleus at roughly equilibration time to be a “pancake” of thickness about 2 fm. The volume of the plasma sample can then be computed in an elementary way using the formula for the area of a lens, and so the angular momentum density can be computed. We find that, for $\sqrt{s_{\text{NN}}} = 200$ GeV collisions at $C = 20\%$ centrality, the angular momentum density is approximately given by

$$\alpha(\sqrt{s_{\text{NN}}} = 200 \text{ GeV}, C = 20\%) \approx \frac{870}{\text{fm}^3}; \quad (28)$$

we have verified that this result is indeed little affected by modifying the centrality between 20% and 50%: for example, if one repeats the computation in the case of 40% centrality collisions, one obtains $932/\text{fm}^3$, that is, a marginally larger value (which would in fact lead to a marginally stricter bound).

According to [66], the energy density in this case is approximately $10.55/\text{fm}^4$, and so we compute the maximal vorticity, according to equation (24), as

$$\omega_{\text{max}}(\sqrt{s_{\text{NN}}} = 200 \text{ GeV}, C = 20\%) \approx 0.00423 \text{ fm}^{-1}. \quad (29)$$

Using a temperature of approximately 190 MeV [66], we can express the vorticity bound in this case in the form

$$[\overline{\mathcal{P}}_{\Lambda'} + \overline{\mathcal{P}}_{\overline{\Lambda}}](\sqrt{s_{\text{NN}}} = 200 \text{ GeV}, C = 20\%) \leq \approx 0.43\%. \quad (30)$$

This value is well below what can be detected; and, indeed, polarization of Λ and $\overline{\Lambda}$ hyperons *was not observed in experiments at this impact energy* (see the rightmost points in Figure 4 of [11]).

If one repeats this calculation for collisions at an impact energy of 62.4 GeV, one finds that the energy density is of course lower (about $7.59/\text{fm}^4$), and that the angular momentum density also drops, *but more sharply*, to around $271.4/\text{fm}^3$ (it scales approximately linearly with $\sqrt{s_{\text{NN}}}$ [30]): this pattern is seen throughout these calculations. The result is a much less stringent bound,

$$[\overline{\mathcal{P}}_{\Lambda'} + \overline{\mathcal{P}}_{\overline{\Lambda}}](\sqrt{s_{\text{NN}}} = 62.4 \text{ GeV}, C = 20\%) \leq \approx 1.07\%, \quad (31)$$

which begins to approach a level that might be detected; unfortunately the error bars are large in this case (see the second-from-rightmost points in Figure 4 of [11]). The data are in any case consistent with our claim that $\overline{\mathcal{P}}_{\Lambda'} + \overline{\mathcal{P}}_{\overline{\Lambda}}$ can be no larger than this.

At the other extreme, one can consider the collisions studied in the ALICE experiment: here, in the collisions at 2.76 TeV, the energy density [70] is about 2.3 times larger than in

the 200 GeV collisions, but the angular momentum density is about 13.5 times larger for a given centrality; furthermore, the temperature is somewhat higher, roughly 300 MeV. The ALICE investigation [21] considered centrality in two ranges: 15% to 50%, and also 5% to 15%. As before, in the first case we can take 20% to be representative, and then we obtain an extremely severe bound:

$$[\overline{\mathcal{P}}_{\Lambda'} + \overline{\mathcal{P}}_{\overline{\Lambda}'}] (\sqrt{s_{\text{NN}}} = 2.76 \text{ TeV}, C = 20\%) \leq \approx 0.047\%. \quad (32)$$

The other range is interesting, since the data go down to a very low centrality. Here the angular momentum is enormous, but it does not vary monotonically with impact parameter, so this case merits separate investigation. The much larger overlap volume when the impact parameter is small (around 3.5 fm for 5% centrality) makes itself felt here, and we find in this case a slightly *less* stringent bound despite the higher angular momenta:

$$[\overline{\mathcal{P}}_{\Lambda'} + \overline{\mathcal{P}}_{\overline{\Lambda}'}] (\sqrt{s_{\text{NN}}} = 2.76 \text{ TeV}, C = 5\%) \leq \approx 0.056\%. \quad (33)$$

We will discuss this interesting relaxation of the bound at low centralities in the Conclusion. In the context of the ALICE collisions, however, this is still an extremely low value.

Even with the substantial (theoretical and observational) uncertainties here, it is clear that, in all cases, the vorticity bound is completely inconsistent with any observation of hyperon polarization in these experiments (and of course this prediction is even more firm for the collisions at 5.02 TeV [71]). This is entirely consistent with the reported data [21].

In summary, the vorticity bound asserts that global polarization of Λ and $\overline{\Lambda}$ hyperons should certainly not be observable at impact energies of 200 GeV and above. It is consistent with a barely observable polarization (if the uncertainties can be very considerably reduced) in collisions at 62.4 GeV, however.

Let us turn, then, to much *lower* impact energies.

6.2 Collisions at 39, 27, and 19.6 GeV

The STAR collaboration took data at 39, 27, and 19.6 GeV impact energies. We interrupt our investigation at 19.6 GeV because, while data were also taken at still lower impact energies (to be discussed below), it is questionable whether the QGP is actually formed in those cases; this is discussed in detail in [66]. We will not take a stand on this issue, but we find it clearest to focus first on the cases which are not in doubt¹⁸.

In the case of collisions at 39 GeV, with 20% centrality, we find that the angular momentum density α has dropped to around 170/fm³, the energy density ε to 7.25/fm⁴, and so the vorticity bound gives us

$$[\overline{\mathcal{P}}_{\Lambda'} + \overline{\mathcal{P}}_{\overline{\Lambda}'}] (\sqrt{s_{\text{NN}}} = 39 \text{ GeV}, C = 20\%) \leq \approx 1.65\%; \quad (34)$$

the corresponding collisions at 27 GeV have $\alpha \approx 117.5/\text{fm}^3$ and $\varepsilon \approx 5.89/\text{fm}^4$, and so we have

$$[\overline{\mathcal{P}}_{\Lambda'} + \overline{\mathcal{P}}_{\overline{\Lambda}'}] (\sqrt{s_{\text{NN}}} = 27 \text{ GeV}, C = 20\%) \leq \approx 2.00\%. \quad (35)$$

¹⁸The situation in the GSI/FAIR and JINR/NICA experiments may well be very different, see below.

Finally, for collisions at 19.6 GeV we have a still lower angular momentum density of around $85.3/\text{fm}^3$ and an energy density of about $5.6/\text{fm}^4$, leading to

$$[\overline{\mathcal{P}}_{\Lambda'} + \overline{\mathcal{P}}_{\overline{\Lambda}'}] (\sqrt{s_{\text{NN}}} = 19.6 \text{ GeV}, C = 20\%) \leq \approx 2.64\%. \quad (36)$$

The agreement with Figure 4 of [11] (sixth pair from left for 39 GeV, fifth from left for 27 GeV, fourth from left for 19.6 GeV) (of course one has to add the two values shown there at each impact energy) is far better than one was entitled to expect (that is, agreement to within a factor of at best 2). The rate at which the total polarization declines with increasing impact energy is reproduced particularly well.

We notice that the vorticity bound is not only (approximately) satisfied: it appears, in all three cases, to be (approximately) attained, that is, the inequality in (1) could be an equation. It may well be that the bound is attained also in the previous cases we examined; it is just that the bound is so low that the polarization, while present, cannot be detected. We will discuss this observation in more detail, below.

In short: at these impact energies, the vorticity bound relaxes quite dramatically, to the point where global polarization of Λ and $\overline{\Lambda}$ hyperons might be observable; and so it has proved: these are the impact energies for which the evidence for hyperon polarization arising from QGP vorticity is most clear-cut [11].

We conclude this discussion with the following observations related to our earlier discussion of the curvature of the spatial sections in our model. Since the bound is at least approximately attained, we can suppose that the corresponding theoretical values of a and L are actually realised in these cases. For example, let us consider collisions at 39 GeV. Here, as above, $\alpha \approx 170/\text{fm}^3$, $\varepsilon \approx 7.25/\text{fm}^4$, so using equation (22) we have $L_{\omega_{\text{max}}} \approx 28.2 \text{ fm}$, so that in this case (from equation (15)) the Gaussian curvature in this case ranges between -0.00048 and 0.0013 fm^{-2} (the value at the equator), which is negligible for systems of this size¹⁹. We have verified that this is so in every case considered in this work.

Finally, we consider the collisions with the lowest impact energies.

6.3 Collisions at 14.5, 11.5, and 7.7 (and 4.9) GeV

Assuming that the QGP continues to be formed at the lowest impact energies studied in [11] — if this is not the case, then a gauge-gravity approach *cannot be used* — we have the following results.

At 14.5 GeV, $\alpha \approx 63.08/\text{fm}^3$, $\varepsilon \approx 4.56/\text{fm}^4$, and then

$$[\overline{\mathcal{P}}_{\Lambda'} + \overline{\mathcal{P}}_{\overline{\Lambda}'}] (\sqrt{s_{\text{NN}}} = 14.5 \text{ GeV}, C = 20\%) \leq \approx 2.98\%; \quad (37)$$

collisions at 11.5 GeV have $\alpha \approx 50.03/\text{fm}^3$ and $\varepsilon \approx 3.97/\text{fm}^4$, leading to

$$[\overline{\mathcal{P}}_{\Lambda'} + \overline{\mathcal{P}}_{\overline{\Lambda}'}] (\sqrt{s_{\text{NN}}} = 11.5 \text{ GeV}, C = 20\%) \leq \approx 3.32\%; \quad (38)$$

and finally the 7.7 GeV collisions have $\alpha \approx 33.50/\text{fm}^3$ and $\varepsilon \approx 3.00/\text{fm}^4$, giving

$$[\overline{\mathcal{P}}_{\Lambda'} + \overline{\mathcal{P}}_{\overline{\Lambda}'}] (\sqrt{s_{\text{NN}}} = 7.7 \text{ GeV}, C = 20\%) \leq \approx 3.85\%. \quad (39)$$

¹⁹In fact, this curvature is of the order of the square of the angular velocity in this case, that is, it is about the same as the (equally negligible) curvature induced by Lorentz contraction effects (under the assumption of approximate Born rigidity) on the “relativistic rotating disc” mentioned earlier.

Except at 7.7 GeV, the agreement with [11] continues to be rather good. In the 7.7 GeV case, the reported polarization for $\bar{\Lambda}$ hyperons is so much larger than that for Λ hyperons that this case should be viewed with caution (see also [22] and [72]). In any case, as we have stressed, it is problematic whether the QGP can form at such low impact energies and relatively low values of the baryonic chemical potential.

Our results are summarized in Figure 2, which should be compared with Figure 4 of [11] by adding together, in the latter, the values corresponding to the two points at each impact energy.

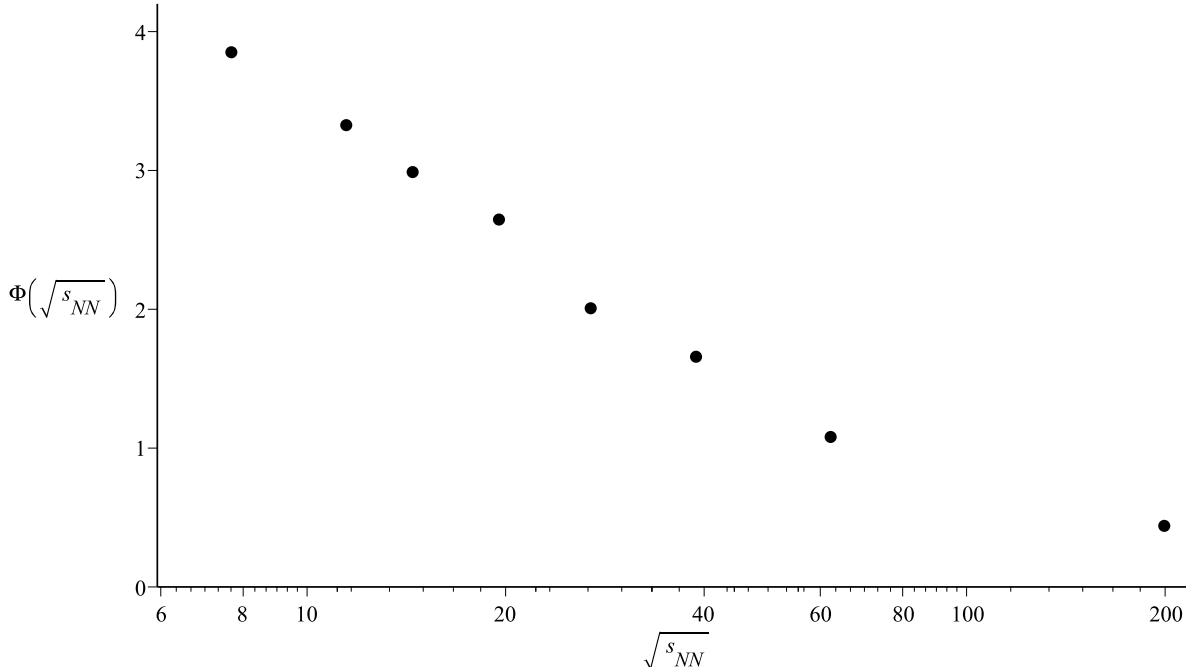


Figure 2: Theoretical upper bounds on total polarization, that is, $[\overline{\mathcal{P}}_{\Lambda'} + \overline{\mathcal{P}}_{\bar{\Lambda}'}](\sqrt{s_{NN}}, C = 20\%) \leq \Phi(\sqrt{s_{NN}}, C = 20\%)$, as a percentage, for collisions at $\sqrt{s_{NN}} = 7.7, 11.5, 14.5, 19.6, 27, 39, 62.4, 200$ GeV and 20% centrality.

7. Attaining the Bound

It is striking that, for all impact energies we have considered but the lowest, the observed vorticities are actually similar in value to the right side of our basic inequality, (1), and not very much smaller than it, as the inequality would permit. Let us take it, as a working hypothesis, that in all experiments in which the impact energy is sufficiently large as to ensure that a QGP is actually formed, and in which the centrality is not extremely small or extremely large (see below), the vorticity attains the largest value permitted by (1). We will see that this allows us to make predictions regarding observations at future facilities, and also to forge a link with certain theoretical ideas regarding the relation between vorticity and angular momentum in these systems.

Obviously, the bound cannot be attained in the case of collisions which are almost exactly central, since the angular momentum density must be close to zero in those cases.

According to [30], the AMPT model mentioned earlier predicts that the angular momentum imparted to the plasma rises from zero, in exactly central collisions, up to a maximum at an impact parameter of about 4 fm, before declining towards zero for larger impact parameters. However, the angular momentum is still very large even for impact parameters somewhat below 4 fm and also for values considerably larger. Based on our findings here, we conjecture that the vorticity bound should be attained, if the QGP is formed, for centralities [67, 68] between 5% and 50%, though a wider range may well be possible.

Consider, for example, collisions at 27 GeV and 5% centrality. Despite the low centrality, the angular momentum density is still around 100 fm^{-3} , significantly higher than the angular momentum density for collisions at 19.6 GeV and 20% centrality (about 85 fm^{-3}). Since the bound is attained in the latter case, it is reasonable to suppose that it is also attained in the former.

Let us see where the hypothesis of the bound being always attained, under the stated conditions, leads us.

We begin with the fact that the GSI/FAIR facility [26] (and similar facilities, also making progress at the time of writing, such as JINR/NICA [28]) are expected to collide heavy ions in such a manner that dense matter at extremely high values of the baryonic chemical potential (perhaps 500 MeV) will be produced. At such values, it may be that the QCD can exist at relatively low temperatures (because the phase transition line bends downward with increasing μ_B ; see in this connection [72]), and so the vorticity bound may be applicable. Assuming this, and assuming also that the bound is attained in collisions with centralities between 5% and 50%, let us proceed.

We consider collisions at perhaps $\sqrt{s_{\text{NN}}} = 4.9 \text{ GeV}$ per pair, generating a quark-gluon plasma with a temperature of around 150 MeV and an energy density of perhaps 2 fm^{-4} ; these are of course strictly speculative estimates. For collisions with 20% centrality we find that, in this case,

$$[\overline{\mathcal{P}}_{\Lambda'} + \overline{\mathcal{P}}_{\overline{\Lambda}'}] (\sqrt{s_{\text{NN}}} = 4.9 \text{ GeV}, C = 20\%) \leq \approx 4.3\%. \quad (40)$$

If the bound is attained, then hyperon polarization should be clearly in evidence in such collisions, if indeed the QGP can form in them. However, we do not expect values of the vorticity very much larger than those already observed.

Another prediction which results if the bound is attained (under the stated circumstances) is as follows. Let us assume that it will be possible, in future, to take polarization data, still at moderate impact energies (19.6 to 39 GeV), but at much lower centralities. (Recall that the ALICE collaboration reports relevant data in the 5 – 15% centrality range; however, this does not mean that such a range can be achieved at lower impact energies.)

This is interesting here because collisions with centralities in roughly the 5% range produce plasmas with the highest angular momenta for a given impact energy (see [30]), so in view of the fact that the vorticity bound is inversely related to α , one might expect a stricter bound in this case. However, the intersection volume is *also* very large for small impact parameters, and (unlike in the case of centralities between 20% and 50%, which have been our main focus of attention in this work) here the two factors do not cancel (because we are near the maximum of the function relating the angular momentum to the impact parameter, so the relation is no longer approximately linear).

It turns out that the tendency of the volume to reduce α outweighs the large value of the angular momentum in this case, so α is actually smaller here, for a given impact energy, than in the cases we considered previously. Assuming that the energy density and temperature are approximately the same in the two cases, the effect is to *raise* the bounds on the total polarization, by a factor of up to about 18%. We saw an example of this in our discussion of the recent ALICE results in Section 6.1. In that case this phenomenon did not matter, because both values were far too small to be detected; here, however, it may be otherwise.

Thus, for example, the upper bound on the total polarization in the case of collisions at 19.6 GeV rises rather significantly from 2.64% to around 3.13% as we shift from 20% down to 5% centrality. If the bound continues to be attained here, then the model predicts that these low-centrality collisions will give rise to observably larger polarizations than their higher-centrality counterparts. If confirmed, this would show clearly that the predicted inverse dependence on angular momentum density is indeed realistic; it would also support the hypothesis that the bound is always attained in these experiments. The predicted bounds, for all of the impact energies considered earlier, and for collisions at 5% centrality, are shown in Figure 3.

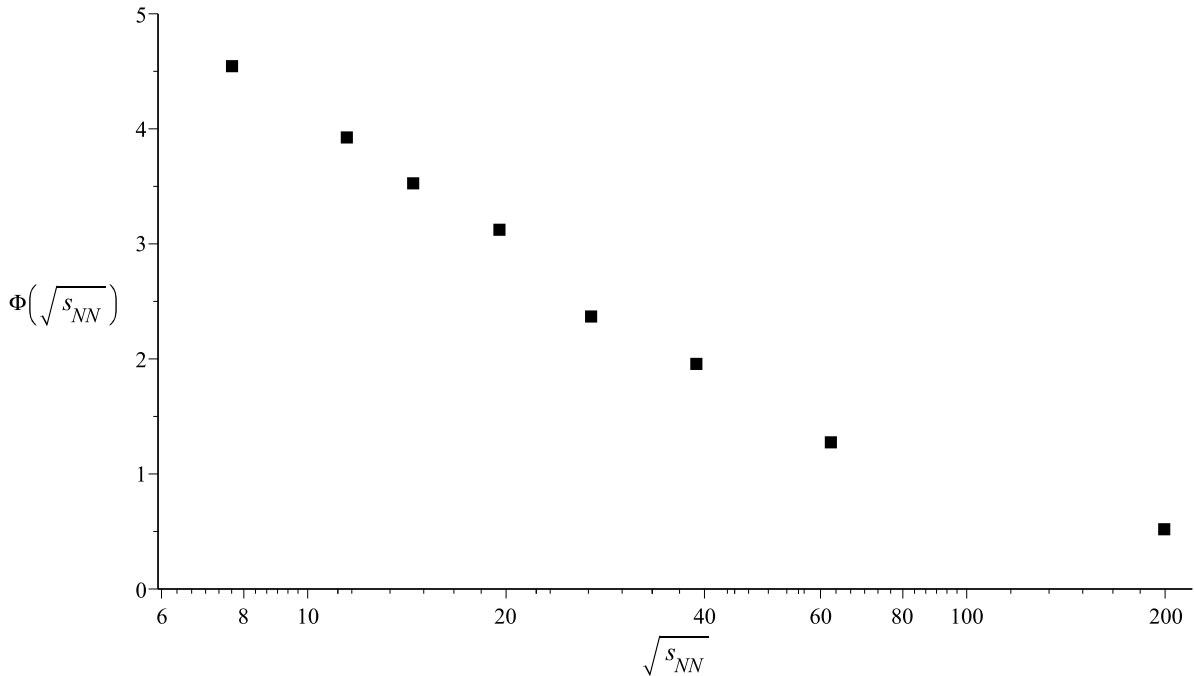


Figure 3: Projected upper bounds on total polarization, that is, $[\overline{\mathcal{P}}_{\Lambda'} + \overline{\mathcal{P}}_{\bar{\Lambda}'}](\sqrt{s_{NN}}, C = 5\%) \leq \Phi(\sqrt{s_{NN}}, C = 5\%)$, as a percentage, for collisions at $\sqrt{s_{NN}} = 7.7, 11.5, 14.5, 19.6, 27, 39, 62.4, 200$ GeV and 5% centrality.

Thus we see that it may be possible to test the hypothesis that the vorticity bound is always attained in reasonably peripheral collisions actually producing a QGP. This hypothesis also has interesting theoretical consequences, however: in particular, it allows us to forge a link with one of the ideas put forward in [30], as follows.

We know from equation (22) that, when the vorticity bound is attained, L is always a fixed multiple, $\varsigma \approx 1.2048$, of a ; and of course we know that a (for fixed centrality)

increases steadily with the impact energy. Thus, in these circumstances, L too increases markedly with impact energy. But we know (see the end of Section 4 above) that L has an interpretation as the “generalized radius of gyration” of the plasma sample. Thus, under the assumption that the vorticity bound continues to be attained as the impact energy increases²⁰, the model predicts that the generalized radius of gyration of the plasma sample (at given centrality) increases with impact energy.

This is related to the claim in [30] that increasing impact energy affects the fluid moment of inertia. Our conclusion is rather more precise: essentially we claim that this statement applies not just to the moment of inertia but also to the radius of gyration (that is, to the moment of inertia *per unit “mass”*). In the holographic model, then, the relevant change with increasing impact energy is in the distribution of matter in QGP vortices, rather than in the energy density. This agrees with the suggestions put forward in [33, 34], which may explain *why* the moment of inertia is (in effect) so sensitive to the impact energy. Clearly this point demands clarification.

To summarize: if the bound is always attained in the experiments, then the holographic model explains the observed decline in the global polarizations with impact energy by implying that the generalized radius of gyration increases with impact energy at fixed centrality. The precise relation expresses the generalized radius of gyration as a linear function of the ratio of the angular momentum density to the energy density; and holography computes the constant of proportionality as $\varsigma \approx 1.2048$.

8. Conclusion

The existence of *some* kind of bound on vorticity should occasion no surprise: the vortex has to resist a centrifugal force in order to sustain itself for a reasonably long interval of time. The question is whether the bound can be implemented in practice (it should depend, in some simple way, on a small number of readily accessible observational parameters); also, to be useful, it should be markedly more restrictive than expected on the basis of obvious constraints such as those imposed by causality.

We have identified a bound, given by inequality (1), which is precisely of this sort. The bound depends on only two readily extracted parameters, the energy density ε and the angular momentum density α ; it is very restrictive, and, crucially, it becomes steadily more so as the impact energy increases.

The agreement of Figure 2 with Figure 4 of [11], apart from one outlier, is surprising; indeed it is remarkable that the trend is even in the correct (downward) direction. The fact that it suggests, correctly, that hyperon polarization associated with QGP vorticity should be observable at impact energies up to around 39 GeV, and not at higher energies, might almost be called startling.

In view of all of the theoretical and observational uncertainties, however, one should not read too much into this. If one could *prove* that QCD itself has a holographic dual, then our results would give grounds for asserting that the holographic vorticity bound reflects a fundamental property of the QGP; but that is not yet the case. Our results do

²⁰This is indeed an additional assumption, beyond the mere existence of a bound: and one notes that, without it, we have no basis for asserting that L must increase as a increases. The existence of a vorticity bound and the increase of L with a are logically independent.

make it reasonable, however, to conjecture that a vorticity bound does exist, and that its mathematical form is similar to that of (1). Holography produces a very specific value for the constant \varkappa ; perhaps this can be improved by more sophisticated considerations. At least we have a concrete basis for further investigations by other methods.

If we assume that the vorticity bound continues to be satisfied, then the model allows us to make definite predictions for the results of future experiments: first, that the vorticity will be observed to be still larger in the beam energy scans, if these reach the regions of the quark matter phase diagram where the QGP can exist at relatively low temperatures, and, second, that it will also be larger if observations can be taken at much smaller centralities. Confirmation of these predictions would be evidence that some kind of bound, similar perhaps to (1), does indeed exist.

We close with a more general observation. It has been said [73] that one reason for the importance of the KSS bound [49, 50] on the dynamic viscosity η of the QGP given its entropy density s is that it gives a benchmark: saying that η is “small” now *means* that η is not far above $s/4\pi$.

We would like to suggest that the vorticity bound might be used to establish a similar benchmark here: instead of saying that the overall value of the vorticity reported in [11], $9 \pm 1 \times 10^{21} \cdot \text{s}^{-1}$, is “large” (meaning that it is large when compared with vorticities attained in other, vastly more extended and very different systems), we might assert that the vorticities attained in these experiments are “large” because, as we have shown, they are of the order of $0.3487 \varepsilon/\alpha$ for collisions at nearly all impact energies — in other words, they are about as large as they can be, if the bound is correct. Since it is probable that no other substance can sustain vortices at such high angular momentum densities, one can say that the vorticities reported by the STAR collaboration may, in this sense, be the largest possible for any substance. In any case, it might possibly be useful, with future more precise data, to report vorticities at a given impact energy by comparing them with the putative maximum possible value in given circumstances.

Acknowledgements

The author thanks Dr Soon Wanmei for valuable discussions.

References

- [1] Zuo-Tang Liang, Xin-Nian Wang, Globally polarized quark-gluon plasma in non-central A+A collisions, Phys.Rev.Lett. 94 (2005) 102301, Erratum-ibid. 96 (2006) 039901, arXiv:nucl-th/0410079
- [2] F. Becattini, F. Piccinini, J. Rizzo, Angular momentum conservation in heavy ion collisions at very high energy, Phys.Rev.C77:024906,2008, arXiv:0711.1253 [nucl-th]
- [3] Xu-Guang Huang, Pasi Huovinen, Xin-Nian Wang, Quark Polarization in a Viscous Quark-Gluon Plasma, Phys. Rev. C84, 054910(2011), arXiv:1108.5649 [nucl-th]
- [4] D.J. Wang, Z. Néda, L.P. Csernai, Viscous potential flow analysis of peripheral heavy ion collisions, Phys. Rev. C 87, 024908 (2013), arXiv:1302.1691 [nucl-th]

- [5] D.E. Kharzeev, J. Liao, S.A. Voloshin, G. Wang, Chiral magnetic and vortical effects in high-energy nuclear collisions – A status report, *Prog.Part.Nucl.Phys.* 88 (2016) 1, arXiv:1511.04050 [hep-ph]
- [6] Wei-Tian Deng, Xu-Guang Huang, Vorticity in Heavy-Ion Collisions, *Phys.Rev.* C93 (2016) 064907, arXiv:1603.06117 [nucl-th]
- [7] Long-Gang Pang, Hannah Petersen, Qun Wang, Xin-Nian Wang Vortical fluid and Λ spin correlations in high-energy heavy-ion collisions, *Phys.Rev.Lett.* 117 (2016) no.19, 192301, arXiv:1605.04024 [hep-ph]
- [8] F. Becattini, I. Karpenko, M. Lisa, I. Upsal, S. Voloshin, Global hyperon polarization at local thermodynamic equilibrium with vorticity, magnetic field and feed-down, *Phys. Rev. C* 95, 054902 (2017), arXiv:1610.02506 [nucl-th]
- [9] M.A.Zubkov, Hall effect in the presence of rotation, arXiv:1801.05368 [hep-ph]
- [10] V.A. Okorokov (on behalf of the STAR Collaboration), Highlights from STAR heavy ion program, *EPJ Web Conf.* 158 (2017) 01004, arXiv:1710.05313 [nucl-ex]
- [11] STAR Collaboration (L. Adameczyk et al.), Global Λ hyperon polarization in nuclear collisions: evidence for the most vortical fluid, *Nature* 548, 62 (2017), arXiv:1701.06657 [nucl-ex]
- [12] Iu. Karpenko, F. Becattini, Study of Lambda polarization in relativistic nuclear collisions at $\sqrt{s_{NN}} = 7.7 - 200$ GeV, *Eur. Phys. J. C* (2017) 77: 213, arXiv:1610.04717 [nucl-th]
- [13] Hui Li, Long-Gang Pang, Qun Wang, Xiao-Liang Xia, Global Λ polarization in heavy-ion collisions from a transport model, *Phys. Rev. C* 96, 054908 (2017), arXiv:1704.01507 [nucl-th]
- [14] Iu. Karpenko, F. Becattini, Vorticity in the QGP liquid and Λ polarization at the RHIC Beam Energy Scan, *Nucl.Phys.* A967 (2017) 764, arXiv:1704.02142 [nucl-th]
- [15] Hui Li, Hannah Petersen, Long-Gang Pang, Qun Wang, Xiao-Liang Xia, Xin-Nian Wang, Local and global Λ polarization in a vortical fluid, *Nucl.Phys.* A967 (2017) 772, arXiv:1704.03569 [nucl-th]
- [16] Qun Wang, Global and local spin polarization in heavy ion collisions: a brief overview, *Nucl.Phys.* A967 (2017) 225, arXiv:1704.04022 [nucl-th]
- [17] Yuji Hirono, Chiral magnetohydrodynamics for heavy-ion collisions, *Nucl.Phys.* A967 (2017) 233, arXiv:1705.09409 [hep-ph]
- [18] Yifeng Sun, Che Ming Ko, Lambda hyperon polarization in relativistic heavy ion collisions from the chiral kinetic approach, *Phys.Rev.* C96 (2017) no.2, 024906, arXiv:1706.09467 [nucl-th]
- [19] Sergei A. Voloshin, Vorticity and particle polarization in heavy ion collisions (experimental perspective), arXiv:1710.08934 [nucl-ex]

- [20] STAR Collaboration: B.I. Abelev, I. Selyuzhenkov, et al., Global polarization measurement in Au+Au collisions, Phys.Rev.C76:024915,2007, arXiv:0705.1691 [nucl-ex]
- [21] Bedangadas Mohanty for the ALICE Collaboration, Measurements of spin alignment of vector mesons and global polarization of hyperons with ALICE at the LHC, arXiv:1711.02018 [nucl-ex]
- [22] Shuzhe Shi, Kangle Li, Jinfeng Liao, Searching for the Subatomic Swirls in the CuCu and CuAu Collisions, arXiv:1712.00878 [nucl-th]
- [23] Ludwik Turko, for the NA61/SHINE Collaboration, Looking for the phase transition - recent NA61/SHINE results, arXiv:1801.06919 [hep-ex]
- [24] Xiaofeng Luo, Nu Xu, Search for the QCD Critical Point with Fluctuations of Conserved Quantities in Relativistic Heavy-Ion Collisions at RHIC : An Overview, arXiv:1701.02105 [nucl-ex], Nucl. Sci. Tech. 28, 112 (2017)
- [25] H. Petersen, Beam energy scan theory: Status and open questions, Nucl.Phys. A967 (2017) 145, arXiv:1704.02904 [nucl-th]
- [26] CBM Collaboration: T. Ablyazimov et al., Challenges in QCD matter physics - The Compressed Baryonic Matter experiment at FAIR, Eur. Phys. J. A 53 (2017) 60, arXiv:1607.01487 [nucl-ex]
- [27] Declan Keane, The Beam Energy Scan at the Relativistic Heavy Ion Collider, J.Phys.Conf.Ser. 878 (2017) no.1, 012015
- [28] V.D. Kekelidze, NICA project at JINR: status and prospects, Journal of Instrumentation 12 C06012 (2017)
- [29] B. Betz, M. Gyulassy, G. Torrieri, Polarization probes of vorticity in heavy ion collisions, Phys. Rev. C76, 044901 (2007), arXiv:0708.0035 [nucl-th]
- [30] Y. Jiang, Z.-W. Lin, J. Liao, Rotating quark-gluon plasma in relativistic heavy ion collisions. Phys. Rev. C94, 044910 (2016), arXiv:1602.06580 [hep-ph]
- [31] Iurii Karpenko, Francesco Becattini, Study of Lambda polarization at RHIC BES and LHC energies, arXiv:1710.09726 [nucl-th]
- [32] F. Becattini, Polarization in relativistic heavy ion collisions: a theoretical perspective, arXiv:1711.08780 [nucl-th]
- [33] Xiao-Liang Xia, Hui Li, Qun Wang, Some aspects of global Lambda polarization in heavy-ion collisions, arXiv:1712.02677 [nucl-th]
- [34] Xiao-Liang Xia, Hui Li, Ze-bo Tang, Qun Wang, Probing vorticity structure in heavy-ion collisions by local Λ polarization, arXiv:1803.00867 [nucl-th]
- [35] Yu. B. Ivanov, A. A. Soldatov, Vortex rings in fragmentation regions in heavy-ion collisions at $\sqrt{s_{NN}} = 39$ GeV, arXiv:1803.01525 [nucl-th]

- [36] Brett McInnes, Holography of the QGP Reynolds Number, Nucl.Phys. B921 (2017) 39, arXiv:1702.02276 [hep-th]
- [37] V. Skokov, A.Yu. Illarionov, V. Toneev, Estimate of the magnetic field strength in heavy-ion collisions, Int.J.Mod.Phys. A24 (2009) 5925, arXiv:0907.1396 [nucl-th]
- [38] Wei-Tian Deng, Xu-Guang Huang, Event-by-event generation of electromagnetic fields in heavy-ion collisions, Phys. Rev. C 85 044907 (2012), arXiv:1201.5108 [nucl-th]
- [39] *Strongly interacting matter in magnetic fields*, Eds. D. Kharzeev, K. Landsteiner, A. Schmitt, H.-U. Yee, Lect. Notes Phys. 871, 1 (2013), arXiv:1211.6245[hep-ph]
- [40] Kirill Tuchin, Particle production in strong electromagnetic fields in relativistic heavy-ion collisions, Adv.High Energy Phys. 2013 (2013) 490495, arXiv:1301.0099 [hep-ph]
- [41] Gergely Endrodi, Critical point in the QCD phase diagram for extremely strong background magnetic fields, JHEP 1507 (2015) 173, arXiv:1504.08280 [hep-lat]
- [42] Xu-Guang Huang, Electromagnetic fields and anomalous transports in heavy-ion collisions — A pedagogical review, Rept.Prog.Phys. 79 (2016) 076302, arXiv:1509.04073 [nucl-th]
- [43] Koichi Hattori, Xu-Guang Huang, Novel quantum phenomena induced by strong magnetic fields in heavy-ion collisions, Nucl.Sci.Tech. 28 (2017) 26, arXiv:1609.00747 [nucl-th]
- [44] Brett McInnes, A Rotation/Magnetism Analogy for the Quark Plasma, Nucl.Phys. B911 (2016) 173, arXiv:1604.03669 [hep-th]
- [45] Ashutosh Dash, Victor Roy, Bedangadas Mohanty, Magneto-Vortical evolution of QGP in heavy ion collisions, arXiv:1705.05657 [nucl-th]
- [46] Makoto Natsuume, AdS/CFT Duality User Guide, Lect.Notes Phys. 903 (2015), arXiv:1409.3575 [hep-th]
- [47] Veronika E. Hubeny, The AdS/CFT Correspondence, Class.Quant.Grav. 32 (2015) 124010, arXiv:1501.00007 [gr-qc]
- [48] Oliver DeWolfe, TASI Lectures on Applications of Gauge/Gravity Duality, arXiv:1802.08267 [hep-th]
- [49] P.Kovtun, D.T.Son, A.O.Starinets, Viscosity in Strongly Interacting Quantum Field Theories from Black Hole Physics, Phys.Rev.Lett. 94 (2005) 111601, arXiv:hep-th/0405231
- [50] D. T. Son, A. O. Starinets, Viscosity, Black Holes, and Quantum Field Theory, Ann.Rev.Nucl.Part.Sci.57:95-118,2007, arXiv:0704.0240 [hep-th]

- [51] Jussi Auvinen, Iurii Karpenko, Jonah E. Bernhard, Steffen A. Bass, Revealing the collision energy dependence of η/s in RHIC-BES Au+Au collisions using Bayesian statistics, Nucl.Phys. A967 (2017) 784, arXiv:1704.04643 [nucl-th]
- [52] Steffen A. Bass, Jonah E. Bernhard, J. Scott Moreland, Determination of Quark-Gluon-Plasma Parameters from a Global Bayesian Analysis, Nucl.Phys. A967 (2017) 67, arXiv:1704.07671 [nucl-th]
- [53] Brett McInnes, A Holographic Bound on Cosmic Magnetic Fields, Nucl. Phys. B 892 (2015) 49, arXiv:1409.3663 [hep-th]
- [54] A. Nata Atmaja, K. Schalm, Anisotropic Drag Force from 4D Kerr-AdS Black Holes, JHEP 1104:070,2011, arXiv:1012.3800 [hep-th]
- [55] Brett McInnes, Jet Quenching in The Most Vortical Fluid: A Holographic Approach, arXiv:1710.07442 [hep-ph]
- [56] Marco M. Caldarelli, Guido Cognola, Dietmar Klemm, Thermodynamics of Kerr-Newman-AdS Black Holes and Conformal Field Theories, Class.Quant.Grav. 17 (2000) 399, arXiv:hep-th/9908022
- [57] G.W. Gibbons, M.J. Perry, C.N. Pope, The First Law of Thermodynamics for Kerr-Anti-de Sitter Black Holes, Class.Quant.Grav.22:1503-1526,2005, arXiv:hep-th/0408217
- [58] Shubhalaxmi Rath, Binoy Krishna Patra, One-loop QCD thermodynamics in a strong homogeneous and static magnetic field, JHEP 1712 (2017) 098, arXiv:1707.02890 [hep-th]
- [59] David Kastor, Sourya Ray, Jennie Traschen, Enthalpy and the Mechanics of AdS Black Holes, Class.Quant.Grav.26:195011,2009, arXiv:0904.2765 [hep-th]
- [60] Clifford V. Johnson, Holographic Heat Engines, Class. Quant. Grav. 31 (2014) 205002, arXiv:1404.5982 [hep-th]
- [61] Brian P. Dolan, Black holes and Boyle's law – the thermodynamics of the cosmological constant, Mod.Phys.Lett. A30 (2015) no.03n04, 1540002, arXiv:1408.4023 [gr-qc]
- [62] Sayantani Bhattacharyya, Subhaneil Lahiri, R. Loganayagam, Shiraz Minwalla, Large rotating AdS black holes from fluid mechanics, JHEP 0809:054,2008, arXiv:0708.1770 [hep-th]
- [63] Oyvind Gron, Sigbjorn Hervik, *Einstein's General Theory of Relativity: With Modern Applications in Cosmology*, Springer Science and Business Media, 2007
- [64] M. N. Chernodub, Shinya Gongyo, Effects of rotation and boundaries on chiral symmetry breaking of relativistic fermions Phys. Rev. D 95, 096006 (2017), arXiv:1702.08266 [hep-th]
- [65] Wit Busza, Krishna Rajagopal, Wilke van der Schee, Heavy Ion Collisions: The Big Picture, and the Big Questions, arXiv:1802.04801 [hep-ph]

- [66] Pragati Sahoo, Swatantra Kumar Tiwari, Sudipan De, Raghunath Sahoo, Rolf P. Scharenberg, Brijesh K. Srivastava, Beam Energy Dependence of Thermodynamic and Transport Properties of Strongly Interacting Matter in a Color String Percolation Approach at the Relativistic Heavy Ion Collider, arXiv:1708.06689 [hep-ph]
- [67] W. Broniowski, W. Florkowski, Geometric relation between centrality and the impact parameter in relativistic heavy-ion collisions, Phys.Rev. C65 (2002) 024905, arXiv:nucl-th/0110020
- [68] Sruthy Jyothi Das, Giuliano Giacalone, Pierre-Amaury Monard, Jean-Yves Ollitrault, Relating centrality to impact parameter in nucleus-nucleus collisions, Phys. Rev. C97, 014905 (2018), arXiv:1708.00081 [nucl-th]
- [69] B.B. Back et al., The PHOBOS perspective on discoveries at RHIC, Nucl.Phys.A757:28-101,2005, arXiv:nucl-ex/0410022
- [70] ALICE Collaboration, Measurement of transverse energy at midrapidity in Pb-Pb collisions at $\sqrt{s_{NN}}=2.76$ TeV, Phys. Rev. C 94, 034903 (2016), arXiv:1603.04775 [nucl-ex]
- [71] Alessandro Grelli (for the ALICE Collaboration), ALICE Overview, arXiv:1711.03369 [hep-ex]
- [72] E.E. Kolomeitsev, V.D. Toneev, V. Voronyuk, Vorticity and hyperon polarization at NICA energies, arXiv:1801.07610 [nucl-th]
- [73] Andreas Karch, Recent Progress in Applying Gauge/Gravity Duality to Quark-Gluon Plasma Physics, AIP Conf.Proc. 1441 (2012) 95, arXiv:1108.4014 [hep-ph]